Detection and Confirmation of Ractopamine and Its Metabolites in Horse Urine After Paylean® Administration*

A.F. Lehner†, C.G. Hughes, J.D. Harkins, C. Nickerson, B. Mollett, L. Dirikolu, J. Bosken, F. Camargo, J. Boyles, A. Troppmann, W. Karpiesiuk, W.E. Woods, and **T. Tobin**

Maxwell H. Gluck Equine Research Center and the Department of Veterinary Science, University of Kentucky, Lexington, Kentucky

Abstract

We have investigated the detection, confirmation, and metabolism of the beta-adrenergic agonist ractopamine administered as Paylean to the horse. A Testing Components Corporation enzyme-linked imunosorbent assay (ELISA) kit for ractopamine displayed linear response between 1.0 and 100 ng/mL with an I-50 of 10 ng/mL and an effective screening limit of detection of 50 ng/mL. The kit was readily able to detect ractopamine equivalents in unhydrolyzed urine up to 24 h following a 300-mg oral dose. Gas chromatography–mass spectrometry (GC–MS) confirmation comprised glucuronidase treatment, solid-phase extraction, and trimethylsilyl derivatization, with selected-ion monitoring of ractopamine-*tris*(trimethylsilane) (TMS) *m/z* 267, 250, 179, and 502 ions. Quantitation was elaborated in comparison to a 445 M_w isoxsuprine-*bis*(TMS) internal standard monitored simultaneously. The instrumental limit of detection, defined as that number of ng on column for which signal-to-noise ratios for one or more diagnostic ions fell below a value of three, was 0.1 ng, corresponding to roughly 5 ng/mL in matrix. Based on the quantitation ions for ractopamine standards extracted from urine, standard curves showed a linear response for ractopamine concentrations between 10 and 100 ng/mL with a correlation coefficient $r > 0.99$, whereas standards in the concentration range of 10–1000 ng/mL were fit to a second-order regression curve with $r > 0.99$. The lower limit of detection for ractopamine in urine, defined as the lowest concentration at which the identity of ractopamine could be confirmed by comparison of diagnostic MS ion ratios, ranged between 25 and 50 ng/mL. Urine concentration of parent ractopamine 24 h post-dose was measured at 360 ng/mL by GC–MS after oral administration of 300 mg. Urinary metabolites were identified by electrospray ionization (+) tandem quadrupole mass spectrometry and were shown to include glucuronide, methyl, and mixed methyl-glucuronide conjugates. We also considered the possibility that an unusual conjugate added 113 amu to give an observed *m/z* 415 [M+H] species or two times 113 amu to give an *m/z* 528 [M+H] species with a daughter ion mass spectrum related to the previous one. Sulfate and mixed methyl-sulfate conjugates were revealed following glucuronidase treatment, suggesting that sulfation occurs in combination with glucuronidation. We noted a paired chromatographic peak phenomenon of apparent ractopamine metabolites appearing as doublets of equivalent intensity with nearly identical mass spectra on GC–MS and concluded that this phenomenon is consistent with Paylean being a mixture of RR, RS, SR, and SS diastereomers of ractopamine. The results suggest that ELISA-based screening followed by glucuronide hydrolysis, parent drug recovery, and TMS derivatization provide an effective pathway for detection and GC–MS confirmation of ractopamine in equine urine.

Introduction

Ractopamine, *N*-[2-(4-hydroxyphenyl)-2-hydroxyethyl]-1-methyl-3-(4-hydroxyphenyl)propylamine, is a β-adrenergic agonist marketed under the trade name Paylean, which is approved for use in swine and other livestock as a growth regulator (1). It has a β-hydroxyphenethylamine structure common to many β-adrenergic agonists (Figure 1) and has the property of repartitioning (i.e., the capability of altering muscle lean-to-fat ratios), most likely through some combination of stimulation of lypolysis, stimulation of protein synthesis, or down-regulation of lipogenesis. This results in reduction of fat, increased muscle mass, and improved feed utilization efficiency in swine, cattle, and turkeys (2). Ractopamine promotes protein deposition with little effect on fat deposition in the pig (3,4). Ractopamine introduced through the diet decreases basal plasma insulin concentrations but has no effect on plasma glucose or non-esterified fatty acids. Antilipolytic effects of insulin tend to be augmented, as well. Di-

* Published as Kentucky Agricultural Experiment Station Article #03-14-041 with the approval of the Dean and Director, College of Agriculture and Kentucky Agricultural Experimental Station. Publication #324 from the Equine Pharmacology, Therapeutics and Toxicology Program of the Maxwell H. Gluck Equine Research Center, University of Kentucky, Lexington, KY 40546-0099. Supported by a grant from The Kentucky Racing Commission, Lexington, KY.

† Author to whom correspondence should be addressed: Andreas F. Lehner, 108 Gluck Equine Research Center, Department of Veterinary Science, University of Kentucky, Lexington, KY 40546-0099. E-mail: alehner@uky.edu.

etary ractopamine has been shown to decrease lipolytic responses to fenoterol, evident after four dose treatments, and the hyperinsulinaemic response to fenoterol was also attenuated by feed supplemented with ractopamine. The desensitization of adipose tissue β-adrenergic receptors is consistent with observations that dietary ractopamine has little effect on the rate of fat deposition in the growing pig (4).

Ractopamine treatment results in a stimulation of myofibrillar protein synthesis and elevates absolute rates of protein synthesis and breakdown in biceps femoris muscle in the pig. The result is enhancement of protein accretion in skeletal muscle of pigs (5). In rats, ractopamine increased methionine incorporation in cultured muscle cells (6). Studies in rats indicate that of the four possible ractopamine stereoisomers (RR, RS, SR, and SS), the RR isomer is responsible for the majority of leanness-enhancing effects (7).

Both conjugated and nonconjugated metabolites of ractopamine have been reported in various species. In cattle and sheep, for example, ractopamine residues in urine samples were measured before and after hydrolysis of conjugates. On the last day of extended administration (day 0), concentrations of parent ractopamine in sheep urine were ~10 ng/mL and were below the limit of quantitation (LOQ) (5 ng/mL) two days post-administration. After hydrolysis of conjugates, ractopamine concentrations were ~5300 ng/mL on day 0 and ~180 ng/mL on day 7 post-administration. A similar picture emerged on study of ractopamine concentrations in cattle urine. The data indicate that after the hydrolysis of conjugates, ractopamine should be detectable in urine of sheep as long as seven days after the last exposure to ractopamine and as long as five days after withdrawal in cattle (8).

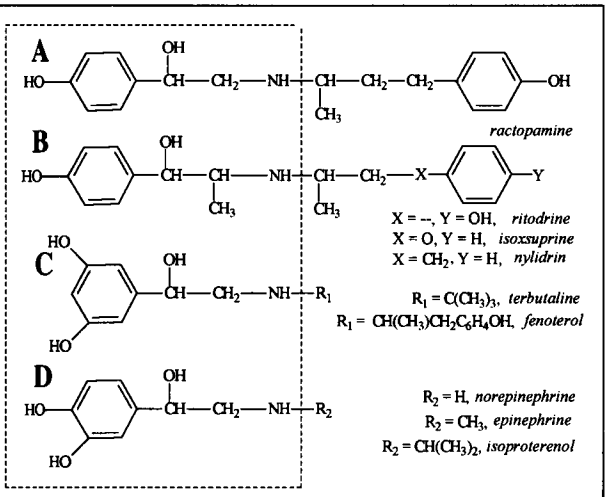

Figure 1. Comparison of ractopamine structure with that of representative β-adrenergic agonists. The common β-hydroxyphenethylamine structure is contained in the box. Ractopamine (A) is closely related to the para-phenolic compounds nylidrin, ritodrine, and isoxsuprine (B), the last of which is only weakly β-adrenergic. Somewhat more distantly related structurally are the strict β2-agonists terbutaline and fenoterol (C), with 3,5-dihydroxy substituents. The pharmacological progenitors of the class of β-adrenergic phenethylamines are the catecholamines (D) displaying 3,4-dihydroxy substituents and including norepinephrine, epinephrine, and isoproterenol, each of which has varying degrees of α-agonist properties, as well.

Conjugate metabolite structures have been studied. In rat bile, for example, approximately 46% of biliary metabolites were identified as a sulfate-ester/glucuronic acid diconjugate of ractopamine. The site of sulfation was at the C-10' phenol (phenol attached to carbinol), and glucuronidation was at the C-10 phenol (phenol attached to methylpropylamine) of ractopamine (9). Monoglucuronides conjugated to the phenols at C-10 (60%) or C-10' (13%) have also been found in turkey poults (10,11). Regioselective glucuronidation occurred favoring the C-10 phenol of ractopamine, with specificity for (1R,3R) and (1R,3S) stereoisomers (11).

Enzyme immunoassay-based detection of ractopamine has been made possible through the availability of commercial enzyme-linked immunosorbent assay (ELISA) kits (12–15); but in at least one case (RS, SR), glucuronides showed only 4% cross-reactivity, whereas (RR, SS) diastereoisomer glucuronides conjugated at the same phenolic group showed no detectable reactivity with the antibody raised against a ractopamine-hemiglutarate (keyhole limpet) hemocyanin conjugate (13). Shelver and Smith (16) have nonetheless been able to demonstrate applicability of the monoclonal antibody-based ELISA for determination of ractopamine residues in sheep and cattle samples.

Ractopamine is an Association of Racing Commissioners, International (ARCI) Class 3 drug (17). It is not a recognized therapeutic medication in the racing horse, however, and it has a significant potential for abuse because it is likely to affect performance. Therefore, improper use of ractopamine needs to be monitored with reliable analytical methodology, as its discovery in performance horses may lead to sanctions against owners or trainers.

The purpose of this study is to determine the metabolism of ractopamine in the horse with the intention of elucidating the structure(s) of target metabolites for mass spectrometric (MS) confirmation of ractopamine administration. High-performance liquid chromatography (HPLC) methods with various detectors exist for ractopamine (8,18); however, electrospray ionization (ESI)-MS is rapidly becoming more widespread with a proliferation of methodologies (19,20). In addition to MS analyses, we determined detectability by ELISA, commercial kits of which are widely available for screening purposes in racing chemistry laboratories.

Experimental

Materials and Methods

Three mature Thoroughbred mares (weighing 564, 542, and 550 kg) were acclimated to their stalls 24 h prior to experimentation. The animals were fed twice a day with grass hay and feed (12%), which was a 50:50 mixture of oats and an alfalfa-based protein pellet. The animals were vaccinated annually for tetanus and were dewormed quarterly with ivermectin (MSD Agvet, Rahway, NJ). A routine clinical examination was performed before each experiment to ensure that the animals were healthy and sound. During experimentation, horses were provided water and hay ad libitum. Each mare served as its own

control. Animals used in these experiments were managed according to the rules and regulations of the Institutional Animal Care Use Committee at the University of Kentucky (Lexington, KY), which also approved the experimental protocol. Ractopamine was administered to horses, orally, in the form of the feed supplement Paylean (Elanco, Charlotte, NC). Doses were 300 mg ractopamine in 3 oz (85 g) Paylean for ELISA and GC–MS analysis and 900 mg in 9 oz (255 g) Paylean for detailed metabolism studies. Urine samples were collected immediately before and at 1, 2, 4, 6, 8, and 24 h after administration using a Harris flush tube (24 Fr diameter × 60-in. length; Seamless, Ocala, FL). Urine samples were divided into aliquots stored at 20C until assayed.

Sample collection and preparation

The ractopamine standard for MS analysis was obtained as a gift from the U.S. Department of Agriculture as ractopamine-HCl. Examination of this material by ESI(+)-MS–MS showed it to consist of ractopamine with no apparent contaminants. Pre- and post-administration urine samples were treated by solid-phase extraction (SPE). The filtrate was then diluted 1:10 with a mixture of 50:50 acetonitrile/0.05% formic acid (aq) for positive-mode MS [ESI(+)-MS–MS]. The mixture was infused 1.2 mL/h via a Harvard syringe pump equipped with a 500-µL Hamilton gas-tight syringe. Infusion was direct into the electrospray probe of the Quattro II MS–MS (Micromass, Beverly, MA).

ELISA detection

Testing Components Corp. (TCC, Collinsville, IL) ractopamine ELISA kits were used to establish the detection limit for ractopamine in equine urine. The assay was performed as specified according to manufacturer's instructions and summarized as follows: a stock solution (1 mg/mL) of ractopamine was prepared in methanol. ELISA standards (0.1–1000 ng/mL) were prepared by dilution of stock with ELISA kit assay buffer. The ELISA kit consisted of microtiter plates, antibody #1, antibody #2 (goat anti-rabbit) concentrate, assay buffer (phosphate buffered saline, pH 7.4), wash solution 20× concentrate, and substrate. The assay was started by pipetting 50 µL standard solutions (and/or samples) into the appropriate wells. Antibody #1 solution (100 µL) was added to each well, followed by gentle mixing and incubation for 30 min at 37°C. The plate was then washed three times with diluted wash solution (300 µL). Freshly diluted antibody #2 (150 µL) was added to each well with gentle mixing. The plate was incubated 30 min at 37°C. The plate was again washed three times as described previously. Substrate (100 µL) was added to each well, and the optical density was read at 650 nm with an ELX800 Microplate Reader (BioTek Instruments, Inc., Winooski, VT) 15 min after initiating the incubation.

β-Glucuronidase hydrolysis

Urine samples were treated for 3 h at 65°C with *Patella vulgata* β-glucuronidase (1000 units of Sigma Type L-II/mL urine diluted to 0.25M sodium acetate, pH 5). The resultant hydrolysates were subjected to SPE as described.

SPE and derivatization

SPE were run on a Speedisk 48 Pressure Processor (SPEware Corp., San Pedro, CA). SPE columns (United Chemical Technologies, Bristol, PA, type CSDAU Clean-screen) were conditioned by adding sequentially 3 mL methanol, 3 mL water, and 1 mL 0.1M sodium phosphate buffer (pH 6.0). Samples were loaded and then the column washed sequentially with 2 mL water, 2 mL 1M acetic acid, and 4 mL methanol. The column was dried with N_2 (20 psi nominal pressure) for 1 min. The column was then eluted with 3 mL dichloromethane/isopropanol/NH_4OH (concentrated) (78:20:2, v/v) into glass tubes. The eluent was evaporated to dryness under a stream of N_2 in a 35–40°C water bath. The residue was dissolved by vortex mixing in 15 µL *N,N*-dimethylformamide and 50 µL *N,O-bis*-(trimethylsilyl)trifluoroacetamide (BSTFA)/1% trimethyl chlorosilane (TMCS) (Pierce Chemicals, Rockville, IL) and then immediately transferred to a micro-injection vial and sealed. Derivatization occurred upon dissolution and/or in the 250°C injector port; incubation at 70°C for 30 min prior to injection was found not to increase the yield of derivative. One microliter was injected into the GC–MS. In cases where ESI(+) MS analysis was the preferred method, resuspension of dried eluents took place directly in 1 mL acetonitrile/0.05% formic acid (1:1).

GC–MS selected ion monitoring (SIM) confirmation

Confirmation of ractopamine in urine following β-glucuronidase hydrolysis, SPE extraction, and trimethylsilane (TMS) derivatization was accomplished by GC–MS SIM. The GC column was an HP-5 MS (30 m × 0.25 mm × 0.25-µm film thickness) operated in the splitless mode with 1 mL/min helium. The GC oven temperature was programmed as follows: 180°C for 2 min, then increased to 280°C at 20°C/min, and held at 280°C for 10 min. Data were collected following a 1-µL injection as follows. Isoxsuprine was chosen as an internal standard because of its similar structure and its uniform and predictable behavior during GC–MS analysis (21). The *m/z* 178 base peak of isoxsuprine-*bis*(TMS) was monitored for quantitation. Ions monitored for the *tris*(TMS)-ractopamine derivative were *m/z* 267 (quantitative ion), 250, 179, and 502, in order of decreasing abundance. The origin of these major ions may be explained by scission of the molecular ion to release TMS-O-C_6H_4-CH-O-TMS (*m/z* 267), $CH_2NHCH(CH_3)CH_2CH_2C_6H_4$-O-TMS (*m/z* 250), or $CH_2C_6H_4O$-TMS (*m/z* 179) fragments, or by simple loss of a methyl group (*m/z* 502). Preparation of the ractopamine standard curve was accomplished by determining the internal standard (*m/z* 178) and ractopamine (*m/z* 267) peak areas for a series of standards (0, 10, 20, 50, 100, 200, 300, 500, and 1000 ng/mL) and plotting the calculated ratio of ractopamine area/internal standard area on the horizontal axis versus concentrations on the vertical axis of a 2D plot. Standard curves prepared in this fashion provided coefficients of determination $R^2 > 0.99$. For GC–MS scanning experiments, the *m/z* 50–700 mass range was scanned at 1.19 scans/s.

MS–MS analysis

Full-scan ESI mass spectra were obtained on analytical standards at 10 µg/mL in 50:50 acetonitrile/0.05% formic acid (aq) (pH ~4) by infusion at 1.2 mL/h via a Harvard syringe pump into the electrospray probe of a Micromass Quattro II MS–MS set in positive ion mode. All spectra were optimized by combination of 1–2 min of uniformly acquired data, background sub-

traction, and peak smoothing.

MS–MS tuning

The MS was tuned for positive ion spectra by direct infusion of 10 ng/µL ractopamine in 50:50 acetonitrile/0.05% formic acid (aq). The peak shape and intensity of the monoprotonated ractopamine *m/z* 302 ion were optimized by adjustment of capillary, high-voltage lens, cone voltage, skimmer lens, and radio frequency lens settings. Skimmer lens offset was left at 5 V. Collision gas (argon) and collision energy were adjusted for collisionally induced dissociation (CID) in the central hexapole by optimizing settings as needed for the second quadrupole. Generally, the collision gas was set to 1–3 × 10^{-3} mbar. Increasing the photomultiplier setting 100–150 V above the regular 650 V sufficiently increased sensitivity. In general, for positive mode, the source cone voltage was set at 24 V, collision energy was –20 V, capillary of the ESI probe was +3.0 kV, skimmer at 2.1 V, and the HV lens was 0.54 kV. The source temperature was set at 120°C.

Results

Ractopamine by electrospray(+)-MS

Ractopamine (301 M_w) readily produced an M+H pseudomolecular ion at *m/z* 302 when dissolved in acetonitrile/0.05% formic acid and examined by ESI(+)-MS, as shown in Figure 2 (top). The daughter ion spectrum of this *m/z* 302 species gave intense responses, particularly at *m/z* 107, 121, 136, and 164 (Figure 2, bottom), and these peaks could be readily assigned in keeping with the structure of ractopamine (see assignments in the figure legend). Urine collected at 4 h post-dose (900 mg) was subjected to β-glucuronidase treatment. The daughter ion spectrum of the SPE *m/z* 302 material is shown in Figure 3 and is an excellent match to that in Figure 2 (bottom). The Figure 2 daughter ion spectrum is also a match for that seen from a pronounced *m/z* 302 peak in the commercial formulation Paylean (data not shown), verifying that no prodrugs or unintended conjugates were present in the feed version of the drug.

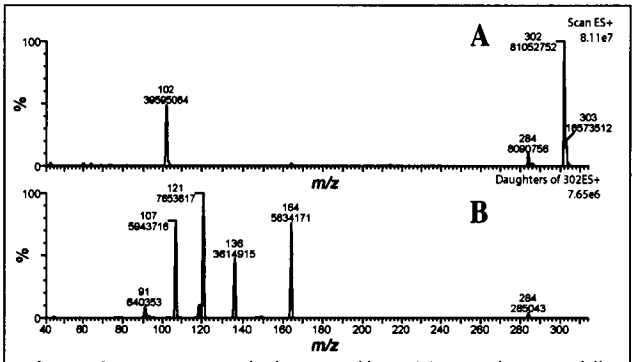

Figure 2. Ractopamine standard examined by ESI(+)-MS and MS–MS: full scan (A) indicating ractopamine $[M+H]^+$ at *m/z* 302 and its dehydrate at *m/z* 284 and daughter ion spectrum (B), 10 µg/mL in acetonitrile/0.05% formic acid (1:1) by direct infusion at 1.2 mL/h. Assignments: 284 = loss of H_2O (benzylic alcohol); 164 = [284 – $CH_2CH_2C_6H_4OH$, either end] + H; 136 = [284 – $HOC_6H_4CH_2CH_2CHCH_3$] + H; 121 = $HOC_6H_4CH_2CH_2$; 119 = 284 – $HOC_6H_4CH_2CH_2CH(NH_2)CH_3$; 107 = $HOC_6H_4CH_2$; 91 = $HOC_6H_4CH_2CH_2$. Minor peaks: 178 = 284 – $CH_2C_6H_4OH$; 149 = $HOC_6H_4CH_2CH_2CHCH_3$; 147 = 284 – [CH_3 and $HOC_6H_4CH_2CH_2CH_3$]; 103 = loss of [[$HOC_6H_4CH_2$ and HOC_6H_4] + H; 74 = $CH_3CH(NH_2CH_2)CH_3$; 58 = $CH_2CH(NH_2)CH_3$; 44 = $CH(NH_2)CH_3$); and unassigned = *m/z* 66, 77, 79, 109.

Ractopamine metabolites by ESI(+)-MS

ESI(+)-mass spectrometry revealed metabolites of ractopamine in urine by comparison of glucuronidase-treated SPE extractions of pre-dose urine (0 h) and that obtained 4 h following a 900-mg dose of ractopamine. Figure 4 displays such a comparison, and new peaks relative to the control are evident at *m/z* 302 (ractopamine) and 284 (instrument-induced dehydration of ractopamine, as seen also in Figure 2, top), as well as 316, 382, 396, 415 (significant enhancement over background), 478, 492, and 528. Figure 5 shows an expansion of the *m/z* 410–570 region of the spectrum, emphasizing these latter species; comparison of the 4-h range with the same spectrum without enzyme treatment (unhydrolyzed) and with 0 h control reveals additional peaks at *m/z* 460, 497, and 500. Substantial reduction in peak height or loss of peaks on enzyme treatment thus suggests glucuronide and/or sulfate involvement for the *m/z* 460, 478, 492, 497, 500, and 528 species.

Table I summarizes the ions seen by ESI(+)-MS and distinguishes whether they were identified in the presence or absence of β-glucuronidase treatment. The table is internally consistent in terms of β-glucuronidase effects because there are

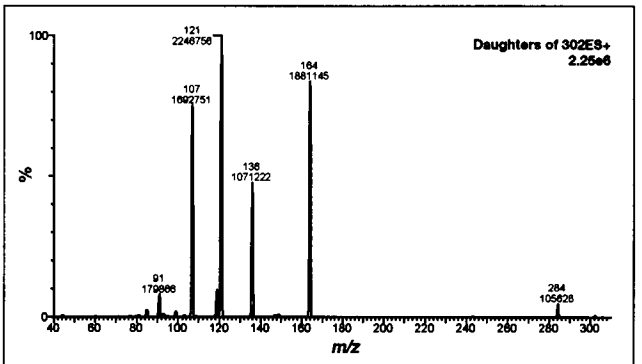

Figure 3. Compound released from 4 h equine urine sample (900-mg dose) by glucuronidase treatment following SPE and matching ractopamine standard by ESI(+)MS–MS (Figure 1).

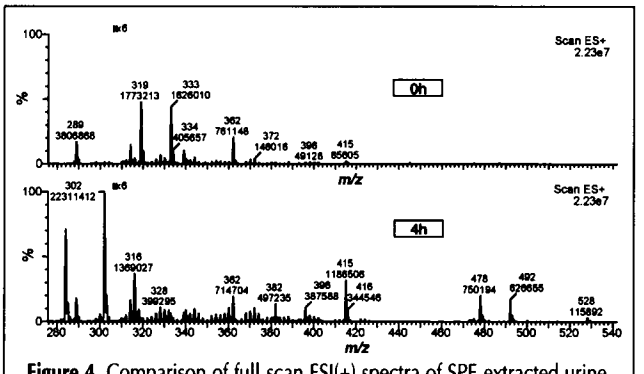

Figure 4. Comparison of full-scan ESI(+) spectra of SPE-extracted urine following glucuronidase hydrolysis, 0 h (top) and 4 h (bottom) after a 900-mg ractopamine dose. Note new peaks at *m/z* 284, 302, 316, 382, 396, 415, and those above 460 in the bottom spectrum.

more lower molecular weight species seen in the presence of β-glucuronidase treatment and more higher molecular weight species without. Species *m/z* 528 and 492 appear to break this rule, however, and incomplete elimination of *m/z* 478 may indicate incomplete hydrolysis under our conditions or an isomeric fraction poorly amenable to hydrolysis.

Examination of the daughter ion spectrum of the *m/z* 478 urine metabolite in the absence of enzyme hydrolysis is presented in Figure 6. The pattern of ion fragments is consistent with that of a glucuronide formed at one of the phenolic hydroxyls, as depicted in the figure on the C-10' hydroxyl (type A) or the C-10 hydroxyl (type B). Peak assignments are consistent with both such structures; and the spectrum could well represent a mixture, although several of the minor peak assignments (e.g., *m/z* 312 and 149) seem to favor the type A structure. The *m/z* 460 ion seen on direct scan (Figure 5, top) thus represents a dehydrate originating from the unconjugated benzylic alcohol of the *m/z* 478 glucuronide(s), as verified by *m/z* 460 in the 478 daughter ion scan and the disappearance or diminution of *m/z* 460 on glucuronidase treatment (Figure 5).

Similar consideration of the *m/z* 492 daughter ions is presented in Figure 7. Its 14 amu difference from the 478 peak, the number of peaks in common between Figures 6 and 7, and the +14 amu differences of ions 492, 474, and 354 with cognates in Figure 6 suggest involvement of methylation, along with glucuronidation. Ready dehydration from this peak to an *m/z* 474 fragment tends to rule out methylation at the benzylic alcohol,

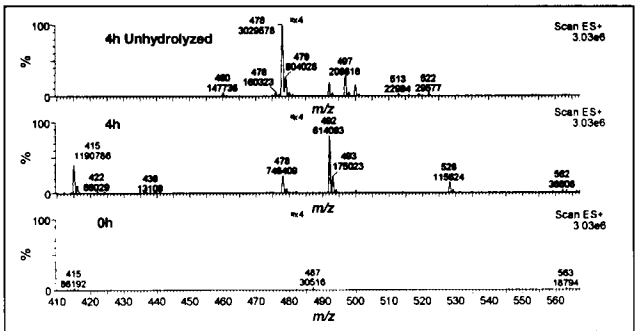

Figure 5. Expansion of high molecular weight region of Figure 4 for study involving 900-mg ractopamine dose. Unhydrolyzed urine (4 h sample, full scan) (top) is compared with hydrolyzed result (middle) and 0 h scan (bottom). Molecular weight species for which the pattern changes suggest glucuronide and/or sulfate involvement include *m/z* 415, 460, 478, 492, 497, 500, and 528.

Table I. Ions $[M+H]^+$ Observed as Most Likely Resulting From Ractopamine Metabolism, Whether in the Presence or Absence of β-Glucuronidase Treatment

With β-Glucuronidase (*m/z*)	Without β-Glucuronidase (*m/z*)
284	
302	302 (trace)
316	
382	
396	
415	
460	
478 (trace)	478
492 (trace)	492
528	

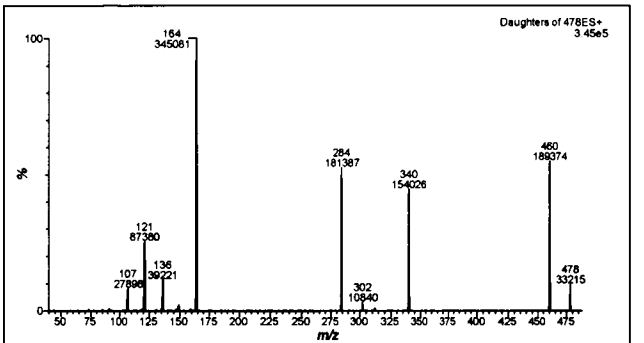

Figure 6. Daughter ion spectrum by ESI(+) of *m/z* 478 ion seen in Figure 5 (top). The pattern is consistent with a glucuronide structure at a phenolic hydroxyl of one of the following types:

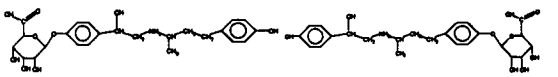

Type A Type B

Assignments: *m/z* 460, loss of H_2O (benzylic alcohol); 340 = [460 – $CH_2CH_2C_6H_4OH$] + H (type A) or [478 – COOH – C_6H_4OH] (type B); 302 = loss of glucuronic acid moiety + H; 284 = 302 minus H_2O (benzylic alcohol); 164 = [284 – $CH_2CH_2C_6H_4OH$]; 136 = [284 – $HOC_6H_4CH_2CH_2CHCH_3$] + H; 121 = $HOC_6H_4CH_2CH_2$; 107 = $HOC_6H_4CH_2$. Minor peaks: 312 = [460 – $HOC_6H_4CH_2CH_2CHCH_3$] + H (type A); 159 = glucuronic acid moiety – OH; 149 = $HOC_6H_4CH_2CH_2CHCH_3$ (type A); 147 = 284 – [CH_3 and $HOC_6H_4CH_2CH_3$]; 131 = glucuronic acid moiety – COOH; 119 = 284 – $HOC_6H_4CH_2CH_2CH(NH_2)CH_3$; 91 = $HOC_6H_4CH_2CH_2$.

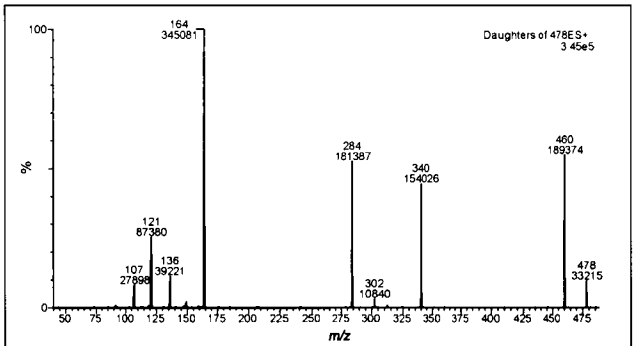

Figure 7. Daughter ion spectrum by ESI(+) of *m/z* 492 ion seen in Figure 5 (top and middle). The pattern is consistent with a glucuronide structure at a phenolic hydroxyl and methylation at the other phenol, yielding one of the following types:

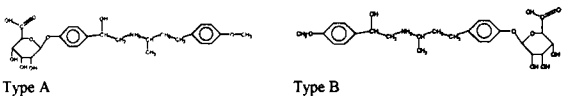

Type A Type B

Assignments: *m/z* 474 = loss of H_2O (benzylic alcohol); 460 = loss of CH_3OH; 354 = 474 – $CH_2C_6H_4OCH_2$ (type A); 340 = 474 $CH_2CH_2C_6H_4OCH_2$ (type A) or 474 – $CH_3OC_6H_4CH{=}CH_2$ (type B); 284 = 474 –[O-glucuronide and CH_3] or 492 [$CH_3CH_2CH_2CH_2$-C_6H_4OCH and CO_2] (type A); 173 = 474 – [O-glucuronide and OCH_3 and phenyl ring ^+H]; 164 = $CH_3CH_2CH_2CH_2C_6H_4OCH_3$ (type A); 136 = $CH_3CH_2C_6H_4OCH_3$ (type A) or $CH_3OC_6H_4CHO$ (type B); 121 = 136–CH_3; 107 = $CH_3OC_6H_4$.

again favoring substitution at the phenolic hydroxyls. Thus, we are given the choice of methylation at C-10/glucuronidation at C-10' (type A) or methylation at C-10'/glucuronidation at C-10 (type B). Although the peak assignments given in the figure legend are consistent with such structures, several (e.g., *m/z* 354 and 164) again favor the type A arrangement. A mixture of the two is nonetheless not ruled out.

Although there is a small trace of the *m/z* 316 ion present in unhydrolyzed urine, its peak intensity increases roughly four-fold following hydrolysis. Because it also bears a +14 amu relationship (this time to ractopamine parent drug), it is an excellent candidate for a simple methylated species, the majority of which was released enzymatically from a mixed glucuronide/methylated metabolite. Daughter ion analysis for *m/z* 316 is presented in Figure 8 and indicates many peaks in common with a ractopamine parent drug, seen on comparison with Figure 2; such common peaks were also seen to varying extents with the glucuronides (Figures 6 and 7). Peak assignments for the *m/z* 316 metabolite are consistent with the possibility of a methylated species on either the C-10 (type A) or C-10' (type B) phenolic alcohols. However, there is no trend in assignments that specifically favors one type over another in this case.

The *m/z* 528 peak is likely related to an additional peak that was first considered to be a matrix ion that had merely increased dramatically in the 4-h urine sample, specifically *m/z* 415 (Figure 4). Figure 9 shows that both the *m/z* 528 and 415 daughter ion spectra share significant ractopamine-related ions, *m/z* 302, 284, and 164. In addition, the *m/z* 528 spectrum includes *m/z* 415 as a daughter ion. If the peaks are related as they seem to be, then *m/z* 415 adds a net 113 amu to [M+H] ractopamine at *m/z* 302, and 528 would then represent the execution of two such additions. Possible structure(s) for this previously unrecognized conjugation or complexation will be presented in the Discussion section.

Figure 10 presents a parent ion scan for the ractopamine *m/z* 164 ion that comprises a $NHCH(CH_3)CH_2CH_2C_6H_4OH$ fragment. Without enzymatic hydrolysis (Figure 10, top), the spectrum shows conjugates *m/z* 478 and 492 (trace), the 478 dehydrate at *m/z* 460, and small amounts of parent drug at *m/z* 302 and its 284 dehydrate. Parent ion scanning following beta-glucuronidase treatment (bottom) reveals these same peaks in considerably changed proportions and confirms the relationship to ractopamine of ions *m/z* 284, 302, 460, 478, and 492, as well as the newly revealed peaks *m/z* 316, 415, and 528.

The remaining pair of ions originally discovered in 4-h post-dose urine in Figure 4 (*m/z* 382 and 396) differ from one another again by +14 amu, implying that they differ by the effects of methylation. Figure 11 reveals that the daughter ion spectra for these ions have many fragmentation events, most of them in common. These spectra are so dissimilar to those of the other metabolites in Figures 3 and 6–9 that they were at first dismissed as coincidental background ions; however, diminished but nonetheless evident ions at *m/z* 107, 121, and 136 indicated a likelihood for relationship to the other metabolites. The straightforward relationship of their molecular weights to sulfate and methylated sulfate, respectively, suggests these as candidate structures, and likely assignments can be made to most of the ions, assuming phenolic sulfation only. One difficulty with these compounds is that they become evident only following β-glucuronidase treatment, as listed in Table I. This implies that their original configuration was likely in combination with a glucuronide, in turn questioning the assignment of methylation at phenolic positions. Note that the benzylic hy-

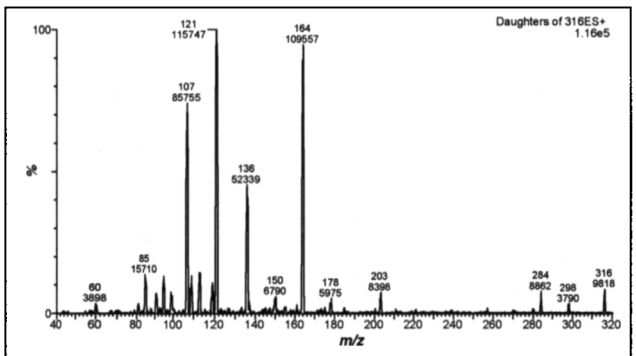

Figure 8. Daughter ion spectrum by ESI(+) of *m/z* 316 ion seen in Figure 4 (bottom). The pattern is consistent with addition of a methyl group, presumably by methylation at the phonolic groups to provide one of the following structures:

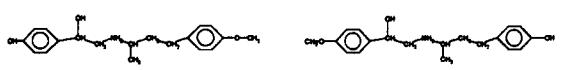

Type A Type B

Assignments: *m/z* 298 = loss of H_2O (benzylic alcohol; 284 = loss of CH_3OH; 203 = loss of $C_5H_4OCH_3$; 178, several possibilities from 316 or 298; 164 = $CH_3CH(NH)CH_2CH_2C_6H_4OH$ (type A) or CH_3CH_2-$CH_2CH_2C_6H_4OCH_3$ (type B); 150 = $CH_3CH_2CH_2CH_2C_6H_4OH$ (type B); 136 = $CH_3CH_2C_6H_4OCH_3$ (type A); 121 = $CH_2CH_2C_6H_4OH$ (type B) or $CH_2C_6H_4OCH_3$ (type A); 107 = $HOC_6H_4CH_2$ or $C_6H_4OCH_3$; 85 = $CH_2NHCH(CH_3)CH_2CH_2$.

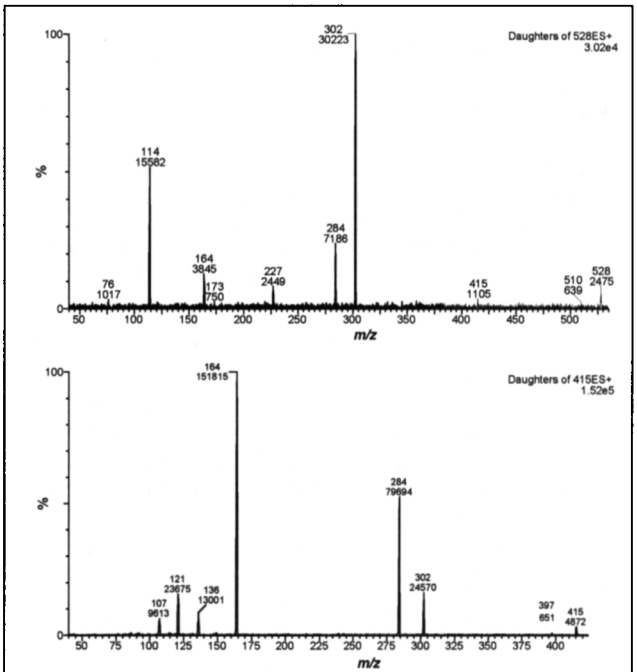

Figure 9. Daughter ion spectrum by ESI(+) of possibly related metabolites *m/z* 528 (top) and *m/z* 415 (bottom) as seen in Figure 5 (middle); these metabolites apparently add an unidentified 113 amu structure either once to make *m/z* 415 or twice to make *m/z* 528.

droxyl group is another alternative for either methylation or perhaps glucuronidation in this case. There is in fact a common tendency to produce the *m/z* 364 ion in both Figure 11 spectra, with lower direct dehydration (to *m/z* 378) from the proposed methylated sulfate, possibly reflecting the effects of blocking the benzylic alcohol position.

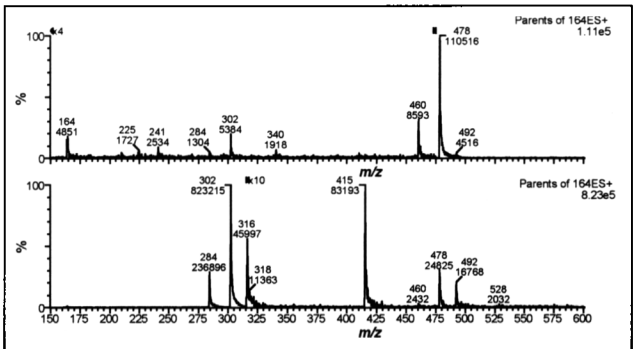

Figure 10. Parent ion scans for the ractopamine *m/z* 164 $NHCH(CH_3)CH_2CH_2C_6H_4OH$ ion before (top) and after (bottom) β-glucuronidase treatment. Metabolites (or dehydrates) thus demonstrated related to ractopamine include ions *m/z* 284, 302, 316, 415, 429, 478, 492, and 528. Note scale enhancements: 4-fold for *m/z* 150–470 region (top) and 10-fold for *m/z* 310–600 region (bottom).

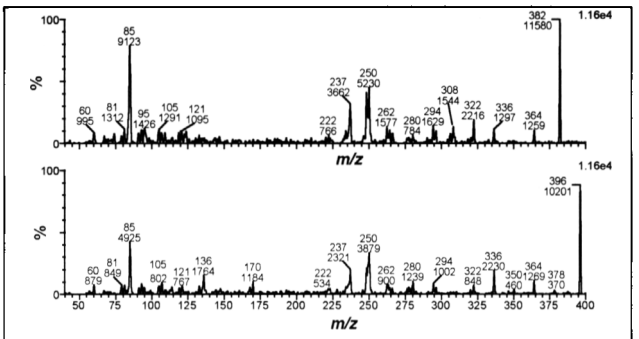

Figure 11. Daughter ion spectrum by ESI(+) of related possible ractopamine metabolites *m/z* 382 (top) and *m/z* 396 (bottom) as seen in Figure 3 (bottom). The top spectrum is consistent with a sulfate metabolite of one of the following likely types:

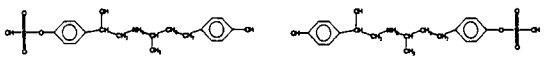

Type A Type B

Assignments: *m/z* 364 = loss of H_2O (benzylic alcohol); 350 = 364 – CH_2; 322 = 350 – C=O; 336 = 364 – CHOH; 322 = 364 – HC=COH; 308 = 350 – CH=C=OH; 294 = 350 – CH-CH=C=OH; 262 = loss of $[CH_2CH_2C_6H_4OH - H]$ (type A); 250 = loss of OH from a desulfated intermediate arising from *m/z* 364; 237 = loss of CH from 250; 121 = $CH_2CH_2C_6H_4OH$ (type A); 105 = $CH_2CH_2C_6H_4$ possibly form desulfated intermediate; 85 = $CH_2NHCH(CH_3)CH_2CH_2$; 60 = $HOCHCH_2NH_2$. Unassigned = *m/z* 280, 248, and 95.

The bottom spectrum is consistent with a sulfate metabolite of one of the following likely types:

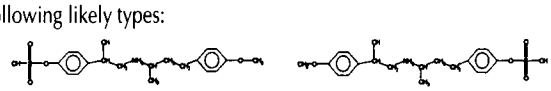

Type A Type B

Assignments: Most of the peaks can be explained by loss of the methyl group, followed by losses described for the simple sulfates. Additional peaks: *m/z* 378 = loss of H_2O (benzylic alcohol); 170 = $CH_2C_4H_4OSO_3$ (type B); 136 = $[CH_3OC_4H_4CHOH - H]$ (type B).

Ractopamine metabolites by GC–MS

Figure 12 presents an examination of ractopamine 4-h postdose metabolites by GC–MS. The top figure shows the total ion chromatogram for derivatized SPE-extracted enzyme-hydrolyzed urine, whereas the middle panel shows a much more simplified pattern derived by performing ion chromatographic analysis of the data in the top panel focusing on ion *m/z* 267. This ion is derived from single internal cleavage of *tris*[TMS]ractopamine beyond the benzylic carbon to provide a TMS-O-C_6H_4CH-O-TMS fragment, although formally three fragmentations (to release TMS and two O-TMS) provides another possible approach. Table II lists predicted molecular weights for ractopamine metabolites and their TMS derivatives, and this provided a guide to interpretation of the data. One discovery was that the principal peak at 9.6 min retention time (RT) is a match to the standard ractopamine, released in this case by β-glucuronidase treatment, and the basis for GC–MS confirmation as described. The highest M_w ion at *m/z* 502 then matches the demethylated *tris*[TMS]ractopamine listed in Table II. The second discovery elicited by the Figure 11 ion chromatography is the occurrence of ractopamine-related metabolites as roughly equivalent area pairs of peaks. This emphasizes the diastereomeric nature of the parent drug, which itself gives the appearance of two nearly superimposed peaks at 9.54 and 9.57 min RT. Table III lists corresponding pairs of peaks based on highly similar mass spectra and their likely structural assignments based on consideration of ESI(+)-MS data and predictions of Table II. The assignments reveal no new metabolites of ractopamine but provide consistent support for the glu-

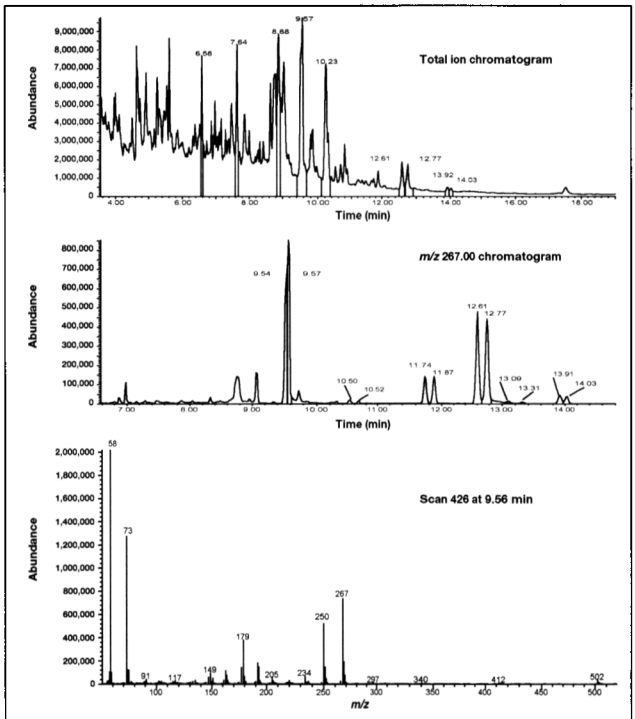

Figure 12. GC–MS analysis of ractopamine-doesd horse urne. The 4 h urine collected after the 900-mg dose was run as described in the Materials and Methods subsection: TIC (top); ion chromatogram for the significant *m/z* 267 ion of ractopamine (middle); and mass spectrum of the 9.56-min peak, demonstrating a M_w mass of 502 and providing a 99% match to library standard of ractopamine-*tris*(TMS) (bottom).

curonide, methyl, and mixed methyl glucuronide metabolites seen by ESI(+)-MS–MS.

ELISA results

A horse was dosed with 300 mg ractopamine orally, and urine samples were collected pre- and post-administration. These urine samples were analyzed by ELISA along with a set of ractopamine standards as described in the Materials and Methods section.

The resultant standard curve for ractopamine in assay buffer (Figure 13, right) was sigmoidal with a substantial linear portion typical of ELISA assays. The linear portion of this curve (1, 5, 10, 50, and 100 ng/mL) had an I-50 of approximately 10 ng/mL and an *r* value of 0.9811. This five-point standard curve was used to estimate the concentration of apparent ractopamine in the dosed horse urine samples (pre- and post-administration) and a panel of five undosed horse urine samples. All urine samples were diluted 1:4 with assay buffer prior to assay. The mean

Table II. Predicted M_w of Ractopamine Metabolites Found During this Study, Their TMS Derivatives, and TMS Derivatives Minus a Single CH_3 Group (–15 amu)

Compound	Mw	TMS	TMS2	TMS3	TMS4	TMS5	TMS6	TMS7
Ractopamine	301	373	445	517	589			
Methylated ractopamine	315	387	459	531				
Ractopamine-*O*-sulfate	381	453	525	597	669			
Methylated ractopamine-*O*-sulfate	395	467	539	611	683			
Ractopamine-*O*-glucuronide	477	549	621	693	765	837	909	981
Methylated ractopamine-*O*-glucuronide	491	563	635	707	779	851	923	
Unknown ractopamine metabolite + 113	414	486	558	630	702			
Unknown ractopamine metabolite + 113 x 2	527	599	671	743	815			
Methylated unknown ractopamine metabolite + 113	428	500	572	644	716			
Loss of a single methyl group from above:								
Ractopamine	286	358	430	502	574			
Methylated ractopamine	300	372	444	516				
Ractopamine-*O*-sulfate	366	438	510	582	654			
Methylated ractopamine-*O*-sulfate	380	452	524	596	668			
Ractopamine-*O*-glucuronide	462	534	606	678	750	822	894	966
Methylated ractopamine-*O*-glucuronide	476	548	620	692	764	836	908	
Unknown ractopmine metabolite + 113	399	471	543	615	687			
Unknown ractopamine metabolite + 113 x 2	512	584	656	728	800			
Methylated unknown ractopamine metabolite + 113	413	485	557	629	701			

Table III. Summary of Results Found by GC–MS Analysis of 4-h Post-Dose Urine Ractopamine Metabolites and Their Likely Assignments

RT by GC–MS (min)	RT of Likely Diastereomeric Cognate (min)	Highest EI Mass Visible (*m/z*)	Other Significant Ions (*m/z*)	Possible Identification
9.54	9.57	502	267, 250, 234, 205, 179, 149, 73	Ractopamine-*tris*(TMS)
10.50	10.52	574	574, 442, 322, 267, 179, 130, 73	Ractopamine-tetrakis(TMS)
11.73	11.87	618	439, 319, 267, 221, 193, 133, 73	Ractopamine-*O*-glucuronide$(TMS)_5$-related fragment involving loss of TMS-O-C_6H_4-CH_2CH=$CHCH_3$
12.61	12.76	527	480, 348, 333, 267, 179, 73	Methylated ractopamine-*O*-glucuronide $(TMS)_4$-related fragment, involving losses of COO-TMS and $CH_2CH_2C_6H_4OCH_3$
13.10	13.31	351	267, 192, 179, 158, 149, 100, 73	Methylated ractopamine$(TMS)_3$-related fragment (e.g., loss of -O-C_6H_5)
13.91	14.05	625	540, 508, 433, 373, 280, 267, 179, 129, 73	Ractopamine-*O*-glucuronide$(TMS)_5$ of opposite orientation to 11.73 & 11.87 min compound, providing a fragment such as CH_2=$NCH(CH_3)CH_2CH_2C_6H_4O$(gluc)$(TMS)_4$

concentration of the blank urine samples (n = 6) was 13.4 ng/mL ± 3.6 standard error of the mean. The dosed horse urine samples were diluted and analyzed by ELISA without enzyme hydrolysis. An estimate of the apparent ractopamine concentrations in these samples is shown in Figure 13 (left). The sigmoidal standard curve for ractopamine over a five-log scale is shown in Figure 13 (right).

The I-50 of ractopamine in buffer for the TCC kit was approximately 10 ng/mL. Indication of a sample as suspected drug containing is usually (i.e., when the maximum o.d. is approximately 1.0) based on approximately 20% inhibition in ELISA work, which for ractopamine in buffer was achieved at about 50 ng/mL on examination of the standard curve. This value may therefore be considered the effective screening limit of detection (LOD) for ELISA. As discussed, the GC–MS LOD for ractopamine in urine was found to be between 25 and 50 ng/mL. Therefore, the GC–MS method reported here should be capable of confirming ractopamine positives detected by ELISA screening.

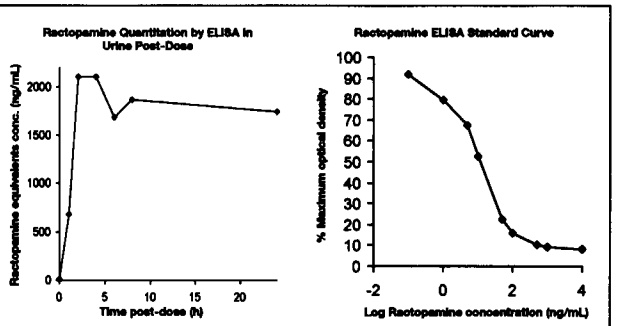

Figure 13. Time course of ractopamine equivalents in urine following a 300-mg oral dose, as determined by ELISA (left); the ractopamine ELISA standard curve (right) was developed over a 5-log range in order to determine the region of linearity best suited for quantitative purposes, namely 1.0–100 ng/mL.

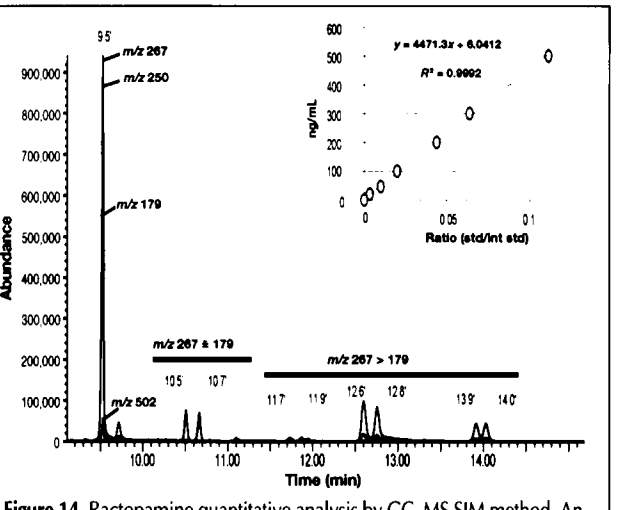

Figure 14. Ractopamine quantitative analysis by GC–MS SIM method. An 8-h post 300-mg oral dose 2-mL urine sample was subjected to glucuronidase hydrolysis, SPE, and derivatization, followed by GC–MS using SIM for selected ions as listed in the Materials and Methods subsection (internal standard not shown). Quantitation following dilution enabled measurement of the recovered ractopamine as 5700 ng/mL. Ractopamine at 9.5' (where ' = minutes retention time) was followed by four pairs of ractopamine-related peaks identified as having roughly equivalent area m/z 267 and 179 peaks (10.5' and 10.7') or by m/z 267, substantially exceeding m/z 179 area (11.7', 11.9', 12.6;, 12.8', 13.9', and 14.0'), with none of these latter peaks displaying nested m/z 250 or 502 peaks as does the 9.5' peak. The insert figure shows a typical standard curve for ractopamine-*tris*(TMS) based on isoxsuprine internal standard.

GC–MS confirmatory method for ractopamine in urine

As described in Figure 12, the *tris*(TMS)-ractopamine derivative elutes at 9.51 min in GC–MS, and the internal standard isoxsuprine-*bis*(TMS) (not shown) elutes at 7.61 min. Of the three major ractopamine ions suitable for quantitative SIM, the m/z 267 ion was found to be free of interference from urinary matrix components at the retention time of ractopamine. A method was thus elaborated that utilized the m/z 267 ion for quantitation, ions m/z 250 and 179 for verification, and the m/z 178 ion of isoxsuprine-*bis*(TMS) as the internal standard quantitation ion. Figure 14 illustrates the application of the confirmatory method to an 8-h post-dose urine sample. The peak of chromatographically merged ractopamine diastereomers at 9.5 min displays nested ion chromatograms at m/z 267 > 250 > 179 > 502. The insert figure shows linearity of the standards between 10 and 500 ng/mL with its corresponding equation and an acceptable R^2 = 0.9992. Paired diastereomeric metabolite peaks seen in Figure 12 (middle) generally display ions m/z 267 and 179 of the ractopamine SIM series and are distinguished as having nearly equivalent m/z 267 and 179 peak areas, or m/z 267 > 179 as indicated.

Figure 15 follows the time course of ractopamine urinary excretion for a selected horse. If the m/z 267 ion is assumed to reflect individual metabolite peaks with equal representation to that from ractopamine, then metabolite concentrations can be readily estimated by comparison to the ractopamine standard curve. These are shown in Figure 15 as well, illustrating their appearance with slightly different time points for peak concentration (e.g., the 12.6–12.8-min component peaks at 6 h vs. ractopamine at 8 h). The 10.5–10.6-min component seems to mirror the ractopamine peak, supporting its assignment as a

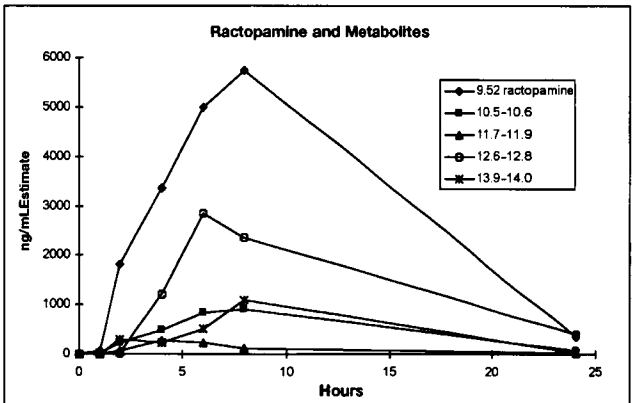

Figure 15. Ractopamine and related metabolites including their trend over time in urine post administration. Ractopamine concentrations (9.52 min RT) were calculated according to the quantitative method described. The others were estimiated based on the recurrence of ion m/z 267 in all compound types; the assumption was made that this related on a 1:1 basis to ractopamine, and a simple ration of m/z 267 abundances was applied to estimate their concentrations. Points shown reflect the average of diastereomeric peaks multiplied by two.

ractopamine-tetrakis(TMS) derivative (Table III). Application of the resultant method enabled identification of ractopamine in enzyme-hydrolyzed equine urine at a concentration of 360 ng/mL 24 h after oral administration of 300 mg of the drug, confirming the appreciable amounts seen by ELISA (Figure 13). Though ractopamine may be detected at relatively low concentrations using the 267 *m/z* ion, confirmation based on the relative abundances of ions *m/z* 250 and 179 limited the capability to confirm its identity to concentrations at approximately 25–50 ng/mL in samples analyzed to date. This is the result of ion *m/z* 267 being free of matrix interference, whereas the diagnostic ions had trace concentration coeluting peaks that varied in concentration with the specific matrix being analyzed. The confirmation limit for ractopamine in urine is thus sufficient for regulatory purposes because it matches that of the ELISA screening test. It is possible that other laboratories attempting to adapt our methods may have significantly lower limits of GC–MS confirmation.

Standard curves based on the *m/z* 267 ion showed a linear response for ractopamine concentrations between 10 and 100 ng/mL with a correlation coefficient $r > 0.99$, whereas standards in the concentration range of 10–1000 ng/mL were fit to a second-order regression curve with $r > 0.99$ (determined with Microsoft Excel 97). Extraction efficiency for the SPE method ranged between 40 and 50%. To determine the instrument lower LOD, signal-to-noise ratios (S/N) were calculated for decreasing amounts of ractopamine-*tris*(TMS) until S/N for the ractopamine quantitative and qualifier ions fell below 3 at 100 pg on-column. The lower LOD for ractopamine in urine, defined as the lowest concentration at which the identity of ractopamine could be confirmed by comparison of diagnostic ion ratios, was 25–50 ng/mL. Criteria for confirmation were those proposed by the Association of Racing Chemists in their *Minimum Criteria for Identification by Chromatography and Mass Spectrometry* (2001). Accuracy and precision were determined by examining runs performed on four different days at concentrations of 50 and 500 ng/mL. Means and coefficients of variation, respectively, were 44.9 ng/mL ± 15.3% and 507.2 ng/mL ± 9.1%.

In order to assess the specificity of the GC–MS SIM method, six unextracted compounds were analyzed at the equivalent of 250 ng/mL with and without ractopamine at the same concentration. Dobutamine, fenoterol, nylidrin, and ritodrine were chosen due to their similarity in structure (Figure 1) or known cross-reactivity in ELISA (12–16), and phenylbutazone and furosemide were chosen for their common occurrence as positives in racing chemistry (W. Carter, personal communication). None of the TMS-derivatives coeluted with ractopamine-*tris*(TMS), with retention times relative to ractopamine-*tris*(TMS) as follows: nylidrin-*bis*(TMS), –1.65 min; ritodrine-*tris*(TMS), –0.68 min; phenylbutazone-TMS, –0.41 min; fenoterol-tetrakis(TMS), –0.1 min; dobutamine-*tris*(TMS), +0.76 min; and furosemide-*bis*(TMS), +1.26 min. None of the compounds had a significant effect on quantitative results for ractopamine. A TMS-derivatized contaminant of ritodrine produced trace chromatographic peaks at the retention time of ractopamine quantitative and qualifier ions. Examination of ion ratios (*m/z* 250, 100%; 267, 240%; 179, 255%) clearly precluded mistaken attribution of these peaks to ractopamine (*m/z* 250, 100%; 267, 110%; 179, 86%), and calculated response based on *m/z* 267 areas at 250 ng/mL was below the minimum level of quantitation for ractopamine.

Discussion

As recognized by the Association of Racing Commissioners, International, ractopamine may have the ability to significantly affect race horse performance, both via its beta-adrenergic agonist properties and its anabolic activities. Therefore, it is of importance to assess screening methodologies such as ELISA tests, as well as the equine metabolism of this drug to provide target structures for mass spectrometric confirmation of its presence in urine samples. ELISA testing with a TCC ractopamine kit provided adequate linearity and sensitivity, and Figure 13 demonstrates the ability of this test to follow the time course of excretion following a single 300-mg oral dose. This dose at less than 1 mg/kg is minimal when compared to that given to pigs (~20 mg/kg) (4). Future ELISA experiments should perhaps be designed to assess the effects of glucuronidase treatment on detectability, given the differential sensitivity of ELISA tests for certain glucuronide stereoisomers (13). GC–MS SIM confirmation was also adequate for quantitation of ractopamine following glucuronidase release of conjugates up to 24 h post-dose and matched the profile of urine excretion provided by ELISA (data not shown).

Equine ractopamine metabolism consisted predominantly of the formation of phase II metabolites in keeping with other species, including turkey (10) where the C-10 glucuronide is divided roughly equally between bile and urine; rat (9) where a C-10'-sulfate/C-10-glucuronide *bis*-conjugate was identified in bile; and cattle, sheep, and ducks (2,8), wherein urine hydrolyzable conjugates have been indirectly described. The general scheme of ractopamine metabolism in the horse is summarized in Figure 16 and presents the simplest interpretations of the data currently available. The figure only considers the nonstereochemical image of ractopamine parent structure, as the absolute placement and three-dimensional configuration of glucuronides, methyl groups, and sulfates cannot be finalized without further detailed investigation. The

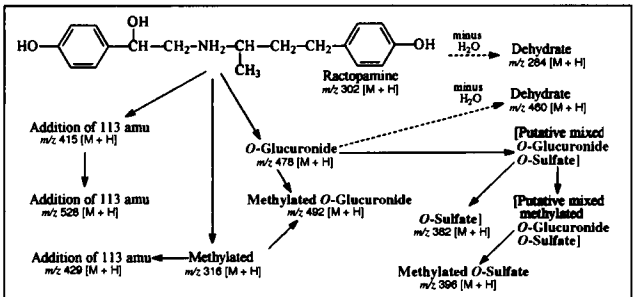

Figure 16. Summary scheme of equine ractopamine metabolism. ESI(+)-MS M+H mass-to-charge ratios are included with each class of structures. Presumed instrumental dehydration events are indicated with a dotted line. Those metabolites adding 113 amu may be covalent or noncovalent complexes (see text). Evidence for the combined addition of 113 amu with methylation should be considered tentative at best.

scheme also demonstrates how the diverse metabolites signified by M+H values *m/z* 316, 382, 396, 415, 429, 478, 492, and 528 can be related to the parent *m/z* 302 M+H, while also accounting for the apparently instrument-derived dehydration products at *m/z* 284 and 460. Other ESI(+) peaks that initially seemed related but for which no support could be obtained included *m/z* 497 and 500 (data not shown). In brief, metabolism of ractopamine is diverse with glucuronidation, sulfation, and methylation routes available to it. We speculate that, despite this observed diversity, there is no particular bias of metabolism type towards any stereochemical configuration, owing to the equivalent peak areas revealed by GC–MS analysis of metabolites arising from the pharmaceutical RR, SS, RS, and SR mixed diastereomeric composition (Figures 12 and 14, Table III).

One unusual aspect of the equine metabolism of ractopamine involved the apparent addition of 113 amu in one or two steps via an unknown mechanism, presumably involving the two phenolic hydroxyl groups. The involvement of the phenols may be supported by similar observations made recently with the structurally related drug isoxsuprine, which has a single phenolic group and appears to add only one 113 amu group according to observations made of urine extracts (Lehner and Bosken, unpublished observations). Review of known generic mechanisms for Phase II conjugation reactions to various functional groups (22) currently include methylation (+14 amu), acetylation (+42 amu), sulfation (+80 amu), succinylation (+101 amu), mercapturic acid formation (+162 amu), and glucuronidation (+176 amu). A review of Merck Index (23) entries in the 112–114 and 130–132 (assuming loss of water) M_w ranges reveals only leucine and isoleucine (M_w 131) as possible conjugating species. Amino acid conjugation generally occurs with amide formation at a drug aromatic carboxylic acid, with glycine (M_w 75) for example, adding a net 57 amu, and conjugation with peptides is a known detoxification mechanisms for exogenous substances in higher plants, for example with phenols in pea seedlings (24). If one assumes that 113 amu conjugation is not an artifact of β-glucuronidase treatment, then one might posit amino acid esterification with leucine or isoleucine as possibilities. This would be unusual not only in that it requires ester formation but offers the difficulty that such conjugates should be subject to blood-borne esterases unless they are unusually stable or formed directly in the kidneys during excretion. The rate of deconjugation of bile acid amidates by cholylglycine hydrolase is dependent on the structure of the amino acid side chain, for example (25).

An alternative would involve noncovalent complexation of ractopamine or methylated ractopamine with the common urine compound creatinine. When the scans in Figure 4 are expanded to include the *m/z* 100–280 region, we observed significant *m/z* 114, corresponding presumably to creatinine (M_w 113) plus a proton. This explanation then requires the presumed metabolites at *m/z* 415 and 528 to be [[ractopamine • creatinine] +H]+1 and [[ractopamine • creatinine$_2$] +H]+1 complexes, respectively. Stacking of the creatinine imidazole ring with the ractopamine phenyl ring may be possible with hydrogen bonding between creatinine's exocyclic amine and the ractopamine phenol group. Drug complexes in biological matrices have been noted (26), and this would be the antithesis of drug-release complexes in pharmaceuticals (27). The only difficulties with this scenario are whether such complexes occur naturally in the urine and that no part of the daughter ion spectrum of the presumed complexes bears any resemblance to the *m/z* 114 daughter ion spectrum (data not shown). More work is required, and deuterium exchange incubations with isoxsuprine complexes (28) may eventually provide additional answers.

References

1. www.elanco.com/paylean.html. Welcome to Paylean.com. *Elanco Animal Health* (2003).
2. D.L. Smith. The pharmacokinetics, metabolism, and tissue residues of beta-adrenergic agonists in livestock. *J. Anim. Sci.* **76:** 173–194 (1998).
3. O. Adeola, R.O. Ball, and L.G.Young. Porcine skeletal muscle myofibrillar protein synthesis is stimulated by ractopamine. *J. Nutr.* **122:** 488–495 (1992).
4. F.R. Dunshea and R.H. King. Responses to homeostatic signals in ractopamine-treated pigs. *Br. J. Nutr.* **73:** 809–818 (1995).
5. W.G. Helferich, D.B. Jump, D.B. Anderson, D.M. Skaerlund, R.A. Merkel, and W.G. Bergen. Skeletal muscle alpha-actin synthesis is increased pretranslationally in pigs fed the phenethanolamine ractopamine. *Endocrinology* **126:** 3096–3100 (1990).
6. P.T. Anderson, W.G. Helferich, L.C. Parkhill, R.A. Merkel, and W.G. Bergen. Ractopamine increases total and myofibrillar protein synthesis in cultured rat myotubes. *J. Nutr.* **120:** 677–683 (1990).
7. E.A. Ricke, D.J. Smith, V.J. Feil, G.L. Larsen, and J.S. Caton. Effects of ractopamine HCl stereoisomers on growth, nitrogen retention, and carcass composition in rats. *J. Anim. Sci.* **77:** 701–707 (1999).
8. D.J. Smith and W.L. Shelver. Tissue residues of ractopamine and urinary excretion of ractopamine and metabolites in animals treated for 7 days with dietary ractopamine. *J. Anim. Sci.* **80:** 1240–1249 (2002).
9. D.J. Smith, J.M. Giddings, V.J. Feil, and G.D. Paulson. Identification of ractopamine hydrochloride metabolites excreted in rat bile. *Xenobiotica* **25:** 511–520 (1995).
10. D.J. Smith, V.J. Feil, and G.D. Paulson. Identification of turkey biliary metabolites of ractopamine hydrochloride and the metabolism and distribution of synthetic [14C]ractopamine glucuronides in the turkey. *Xenobiotica* **30:** 427–440 (2000).
11. D.J. Smith, V.J. Feil, J.K. Huwe, and G.D. Paulson. Metabolism and disposition of ractopamine hydrochloride by turkey poults. *Drug Metab. Dispos.* **21:** 624–633 (1993).
12. W. Haasnoot, P. Stouten, A. Lommen, G. Cazemier, D. Hooijerink, and R. Schilt. Determination of fenoterol and ractopamine in urine by enzyme immunoassay. *Analyst* **119:** 2675–2680 (1994).
13. W.L. Shelver and D.J. Smith. Development of an immunoassay for the beta-adrenergic agonist ractopamine. *J. Immunoassay* **21:** 1–23 (2000).
14. A.L. Wicker, M.P. Turberg, and M.R. Coleman. Evaluation of ractopamine cross-reactivity in several commercially available beta-agonist enzyme immunoassay kits. *Analyst* **120:** 2879–2881 (1995).
15. W.L. Shelver, D.J. Smith, and E.S. Berry. Production and characterization of a monoclonal antibody against the beta-adrenergic agonist ractopamine. *J. Agric. Food Chem.* **48:** 4020–4026 (2000).
16. W.L. Shelver and D.J. Smith. Application of a monoclonal antibody-based enzyme-linked immunosorbent assay for the determination of ractopamine in incurred samples from food animals. *J. Agric. Food Chem.* **50:** 2742–2747 (2002).
17. Association of Racing Commissioners International. Uniform Classification Guidelines for Foreign Substances. Association of Racing Commissioners International, Inc., Lexington, KY, 2003.

http://www.arci.com/publications.html.
18. M.P. Turberg, J.M. Rodewald, and M.R. Coleman. Determination of ractopamine in monkey plasma and swine serum by high-performance liquid chromatography with electrochemical detection. *J. Chromatogr.* **675:** 279–285 (1996).
19. M.I. Churchwell, C.L. Holder, D. Little, S. Preece, D.J. Smith, and D.R. Doerge. Liquid chromatography/electrospray tandem mass spectrometric analysis of incurred ractopamine residues in livestock tissues. *Rapid Comm. Mass Spectrom.* **16:** 1261–1265 (2002).
20. J.P. Antignac, P. Marchand, B. LeBizec, and F. Andre. Identification of ractopamine residues in tissue and urine samples at ultra-trace level using liquid chromatography–positive electrospray tandem mass spectrometry. *J. Chromatogr. B* **774:** 59–66 (2002).
21. J.M. Bosken, A.F. Lehner, C.G. Hughes, W.E. Woods, F.C. Camargo, J.D. Harkins, J. Boyles, and T. Tobin. A GC–MS method for determination of isoxsuprine in biological fluids of the horse utilizing electron impact ionization. *J. Anal. Toxicol.* **28:** 27–34 (2004).
22. J.G. Mandel. *Fundamentals of Drug Metabolism and Drug Disposition,* B.N. LaDu, H.G. Mandel, and E.L. Way, Eds. Robert E. Krieger Publishing Co., Huntington, NY, 1979, pp 149–186.
23. Merck and Co. *Merck Index on CD-ROM,* 13th ed. Merck and Co., Whitehouse Station, NJ, 2001.
24. D. Ugrekhelidze, G.K. Vesitadze, B. Arziani, T. Mithaishvili, and V. Phiriashvili. Detoxification of phenol in annual plant seedlings. *Ecotoxicol. Environ. Safety* **42:** 119–124 (1999).
25. S.M. Huijghebaert and A.F. Hofmann. Influence of the amino acid moiety on deconjugation of bile acid amidates by cholylglycine hydrolase or human fecal cultures. *J. Lipid Res.* **27:** 742–752 (1986).
26. J. Piosik, M. Zdunek, and J. Kapuscinski. The modulation by xanthines of the DNA-damaging effects of polycyclic aromatic agents. Part II. The stacking complexes of caffeine with doxorubicin and mitoxanthrone. *Biochem. Pharmacol.* **63:** 635–646 (2002).
27. P.R. Rege, D.J. Shukla, and L.H. Block. Chitinosan-drug complexes: effects of electrolyte on naproxen release in vitro. *Int. J. Pharmaceutics* **250:** 259–272 (2003).
28. S.A. Lorenz, E.P. Maziaz, and T.D. Wood. Using solution phase hydrogen/deuterium (H/D) exchange to determine the origin of noncovalent complexes observed by electrospray ionization mass spectrometry: in solution or in vacuo? *J. Am. Soc. Mass Spectrom.* **12:** 795–804 (2001).

Manuscript received March 31, 2003;
revision received September 8, 2003.